

# Switching between Aromatic and Antiaromatic 1,3-Phenylene-Strapped [26]- and [28]Hexaphyrins upon Passage to the Singlet Excited State

Young Mo Sung,<sup>†</sup> Juwon Oh,<sup>†</sup> Woojae Kim,<sup>†</sup> Hirotaka Mori,<sup>‡</sup> Atsuhiko Osuka,<sup>\*,‡</sup> and Dongho Kim<sup>\*,†</sup>

<sup>†</sup>Spectroscopy Laboratory for Functional  $\pi$ -Electronic Systems and Department of Chemistry, Yonsei University, Seoul 120-749, Korea

<sup>‡</sup>Department of Chemistry, Graduate School of Science, Kyoto University, Sakyo-ku, Kyoto 606-8502, Japan

**S** Supporting Information

**ABSTRACT:** We have demonstrated aromaticity reversal in the singlet excited states of internally 1,3-phenylene-strapped [26]- and [28]hexaphyrins (**P26H** and **P28H**). **P26H** displays a broad and reduced singlet-excited-state absorption spectrum, whereas **P28H** exhibits a sharp and intense singlet-excited-state absorption spectrum; both are in contrast to the ground-state absorption spectra, strongly indicating aromaticity reversal in the singlet excited state. Furthermore, magnetic and topological indices of aromaticity such as nucleus-independent chemical shift and harmonic oscillator model of aromaticity values for **P26H** and **P28H** also suggest that their singlet excited states become antiaromatic and aromatic, respectively.

During the last several decades, various attempts have been made to quantify the magnitude of aromaticity in  $\pi$ -conjugated cyclic compounds because their chemical stabilities and reactivity should be largely governed by the (anti)-aromaticity.<sup>1,2</sup> In this regard, a number of aromaticity indices representing the magnitude of aromaticity based on quantum-mechanical calculations have been developed, such as topological and magnetic aromatic indices. Topological aromatic indices, such as the harmonic oscillator model of aromaticity (HOMA),<sup>3,4</sup> represent the geometrical changes due to the conjugation effect, while magnetically based aromatic indices, represented by the nucleus-independent chemical shift (NICS),<sup>5,6</sup> exhibit the magnitude of magnetic shielding. Furthermore, in recent years we have found that photophysical properties such as the absorption spectral shapes and fluorescence behaviors, excited-state dynamics, nonlinear optical (NLO) properties, and calculated electronic features can be considered as credible experimental indicators of the aromaticity in a comparable set of  $[4n]/[4n + 2]$  expanded porphyrins.<sup>7,8</sup>

In the meantime, although excited-state aromaticity is one of the most fascinating topics for photostability, chemical reactivity, and applications in photonic devices,<sup>9,10</sup> research on excited-state aromaticity is still in its infancy. In 1972, Baird proposed the aromaticity rule for the lowest triplet state, which was developed by using perturbation molecular orbital theory.<sup>11</sup> He showed that the closed-shell-singlet ground-state aromaticity of annulene is reversed in the lowest triplet state:

annulenes having  $[4n]$   $\pi$  electrons exhibit aromatic features whereas  $[4n + 2]$   $\pi$ -electron systems show antiaromatic features, contrary to their closed-shell-singlet ground states, which is termed aromaticity reversal. To date, there have been many studies related to Baird's rule, including both theoretical and experimental works.<sup>12–25</sup> However, experimental studies to reveal aromaticity reversal by employing a pair of aromatic and antiaromatic congeners having the same molecular framework are a monumental task because it is hard to synthesize stable aromatic and antiaromatic congeners and define the distinct experimental features distinguishing aromatic and antiaromatic molecules. In this regard, we recently demonstrated aromaticity reversal in bis(rhodium) hexaphyrins by analyzing the absorption spectra for transitions between the ground and lowest triplet states with quantum-mechanical calculations, which suggested that spectroscopic results can be evidence of Baird's rule.<sup>24</sup>

Since Baird demonstrated aromaticity reversal in the lowest triplet state in 1972, plenty of theoretical studies have been conducted to extend Baird's rule to the first singlet excited state.<sup>9,14,26,27</sup> In this context, in 2008 Karadakov suggested that the aromaticity of annulene in the lowest singlet excited state also could be reversed relative to the ground state.<sup>26,27</sup> However, to the best of our knowledge, experimental studies to demonstrate the reversal of (anti)aromaticity in the lowest singlet excited state by spectroscopic methods have rarely been reported,<sup>21–23</sup> although significant research has been dedicated to the study of aromaticity in the excited state.

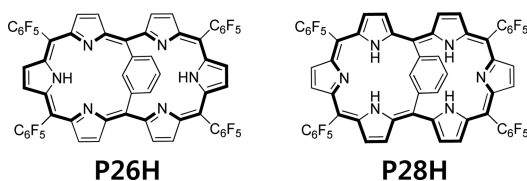
Hexaphyrins, which were employed as a representative comparable set of (anti)aromatic congeners in a previous paper,<sup>24</sup> are among the most suitable molecular systems for investigating aromaticity reversal in the lowest singlet excited state because of their excellent photostability and optical properties as well as the preparation of stable and rigid (anti)aromatic congeners by simple two-electron redox reactions.<sup>8,28,29</sup> Especially, in comparison with aromatic hexaphyrins, their antiaromatic congeners exhibit broad and featureless absorption spectra, an absence of fluorescence, and a one-photon optically dark  $S_1$  state that causes a rapid decay to the ground state.<sup>7,8</sup> Interestingly, the spectral features in the transient absorption (TA) spectra of aromatic and antiaromatic

Received: April 20, 2015

Published: September 4, 2015

expanded porphyrins contrast to each other in a comparable set of  $[4n]/[4n + 2]$  congeners. In this work, we demonstrated the aromaticities of the lowest singlet excited states of [26]- and [28]hexaphyrins by comparison of their photophysical properties. Nevertheless, it has been demonstrated that most *meso*-aryl [28]hexaphyrins tend to be Möbius aromatic or figure-eight nonaromatic ones via structural distortions in the solution phase.<sup>8,29–31</sup> In contrast, internally phenylene-bridged hexaphyrins that are constrained to take spectacles-like conformations, such as [26]hexaphyrin **P26H** and [28]hexaphyrin **P28H** (Chart 1), can be good candidates for studying singlet-excited-state aromaticity.<sup>32</sup>

Chart 1. Molecular Structures of **P26H** and **P28H**



**P26H** and **P28H** exhibit Hückel aromaticity and antiaromaticity, respectively, in their ground states, as probed by  $^1\text{H}$  NMR spectroscopy and NICS calculations.<sup>32</sup> The ground-state absorption spectrum of **P26H** displays sharp and intense spectral features similar to those of aromatic porphyrins, except for large red shifts. On the other hand, **P28H** shows relatively weak and broad absorption spectra up to  $\sim 600$  nm with an extremely weak absorption tail in the NIR region, corresponding to an optically dark state (see the Supporting Information (SI)).

Femtosecond TA spectra of **P26H** exhibited single-exponential decay with a time constant of 160 ps, corresponding to the  $Q_x$  state ( $S_1$ ) lifetime (see the SI). With the aid of global fitting of the whole TA spectrum by singular-value decomposition (SVD), we can evaluate the decay-associated spectrum (DAS) of one transient species, the  $Q_x$  state, as shown in Figure 1. Because the DAS consists of ground-state bleaching (GSB), stimulated emission (SE), and excited-state absorption (ESA), the genuine ESA spectrum for

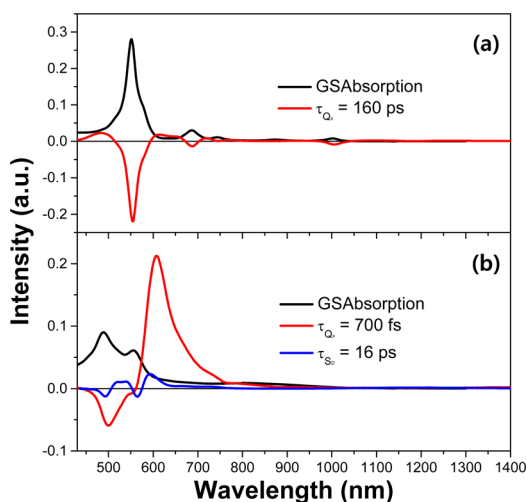


Figure 1. Ground-state absorption (black lines) and decay-associated transient absorption spectra (colored lines) of (a) **P26H** and (b) **P28H** in toluene.

the  $Q_x$  state can be estimated by subtracting the steady-state spectrum, including the ground-state absorption and fluorescence spectra, from the DAS of the  $Q_x$  state (see the SI). Along the same lines, two DASs were obtained for **P28H**, originating from the  $Q_x$  state and the one-photon-forbidden dark state ( $S_D$ ), corresponding to the  $S_2$  and  $S_1$  states, with lifetimes of 700 fs and 16 ps, respectively (Figure 1b). Because of the absence of fluorescence in **P28H**, the ESA spectra of both the  $Q_x$  and  $S_D$  states could be obtained by extraction from the ground-state absorption spectrum and the DAS (see the SI).

In porphyrin-related compounds, strong absorption peaks observed in the ESA spectra can be assigned as transitions from  $Q_x$  to higher singlet excited states ( $S_n$ ) with gerade symmetry according to the selection rule for one-photon optical transitions, because both the B and Q states are of  $E_u$  symmetry.<sup>7</sup> In addition, quantum-chemical calculations of vertical excitation energies gave numerous one-photon dark states with gerade symmetry in the region above the B states in both **P26H** and **P28H**. These energetic and symmetric relationships enabled us to assign all of the observed ESA bands for **P26H** and **P28H** (see the SI).

To comparatively analyze the optical features of the ground and singlet excited states, the extinction coefficients for the ground- and singlet-excited-state absorptions were calculated as shown in Figure 2 (the detailed procedure to evaluate the ESA

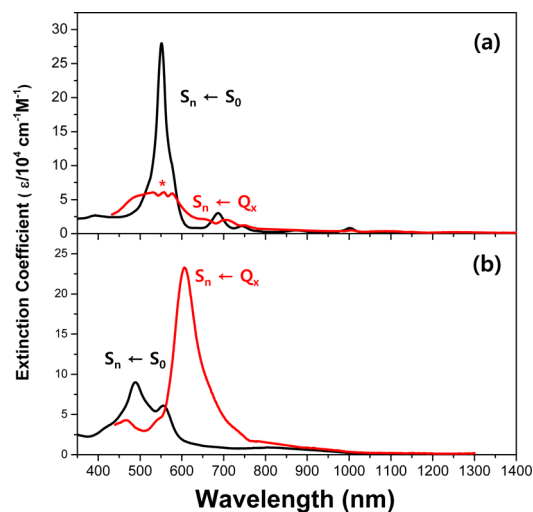


Figure 2. Absorption spectra of the ground states (black lines) and lowest singlet excited states (red lines) of (a) **P26H** and (b) **P28H**. The asterisk (\*) indicates an instrumental error peak due to the different spectral resolutions of the spectrometers employed in the absorption and transient absorption measurements.

is described in the SI). It is noted that the ESA from the  $Q_x$  states of two hexaphyrins was considered herein because the  $S_1$  state originating from a direct HOMO–LUMO transition (gerade–gerade) has much different characteristics than the representative B and Q states in porphyrinoids. By comparison with the ground-state absorption spectrum, the ESA spectrum of the  $Q_x$  state in **P26H** was relatively broad and 4 times weaker in intensity, being quite similar to the typical absorption features observed in antiaromatic porphyrinoids. Therefore, we could propose that the lowest singlet excited state ( $Q_x$  state) of **P26H** presumably becomes antiaromatic. On the other hand, the spectral shape and intensity of the ESA of the  $Q_x$  state in

**P28H** were sharpened and intensified, which could be assumed to be aromatic (Figure 2b). These aspects of spectral changes were nearly similar to those between the ground and lowest triplet states of previous bis(rhodium) hexaphyrins.<sup>18</sup> Thus, it is obvious that the (anti)aromaticity of phenylene-bridged hexaphyrins in the  $Q_x$  state is reversed in comparison with the ground state.

To address the issue of reversed aromaticity of hexaphyrins in the singlet excited state ( $Q_x$  state) relative to the ground state, the calculation of NICS values<sup>3,6</sup> and anisotropy of the induced current density (ACID)<sup>33</sup> maps of (anti)aromatic hexaphyrins were attempted at the B3LYP/6-31g(d,p) level. In this work, we analyzed the aromatic indices in the lowest triplet state instead of the  $Q_x$  state. Previous results for annulenes such as cyclooctatetraene, benzene, and pentafulvene revealed that aromaticity reversal in the lowest triplet state also could be observed in the singlet excited state. Compared with the ground state, the aromaticity indices such as NICS values, magnetic susceptibilities, and energy levels in the singlet excited state are reversed, which is similar to those in the lowest triplet state.<sup>21–23,26,27</sup> Furthermore, our experimental results for **P26H** and **P28H** clearly show reversed features in their  $Q_x$  states relative to the ground state, which is similar to the previous results about aromaticity reversal of rhodium hexaphyrins in the lowest triplet state.<sup>24</sup> Accordingly, we assume that the aromaticity of hexaphyrins in the singlet excited state could have relevance to that in the lowest triplet state. Furthermore, it is difficult to calculate the singlet-excited-state properties of macrocyclic compounds such as hexaphyrins because of the limitation of quantum-mechanical calculations of excited states. Thus, we calculated the NICS values and ACID maps of hexaphyrins in the lowest triplet state instead of those in the lowest singlet excited state. In the case of **P26H**, the average NICS(0) value calculated at the peripheral positions (a and b) was evaluated to be  $-14.99$  ppm in the ground state, which indicates its aromatic character. On the other hand, a positive value ( $+10.51$  ppm) was observed in the  $T_1$  state (see the SI). This result is in good agreement with the aromaticity reversal phenomena upon changing from the ground state to the  $T_1$  state (see the SI). On the other hand, the opposite change of aromaticity was also observed in **P28H**. The NICS(0) value of **P28H** in the  $T_1$  state shows a negative value ( $-16.32$  ppm), while that in the ground state exhibits a positive value ( $+14.76$  ppm). As shown in the SI, averages of the NICS(1) and NICS(3) values at the peripheral sites (a and b) also demonstrate the (anti)aromaticity reversal of **P26H** and **P28H** in the lowest triplet states relative to their ground states. Because the identical signs and similar magnitudes of the NICS values computed at different sites, we can consider that the NICS values of **P26H** and **P28H** reflect the global aromaticity induced by the main  $\pi$ -conjugation pathway rather than local aromaticity triggered by local aromatic rings such as pyrrole or benzene.

The ACID maps are also consistent with the results described above. An ACID map represents a 3D image of the delocalized electron density with a scalar field and illustrates the paramagnetic term of the induced current density when the molecule interacts with an external magnetic field.<sup>33</sup> The general direction of the ring-current flow in the ACID map was inverted from clockwise (aromatic) to counterclockwise (antiaromatic) in the ground and  $T_1$  states of **P26H**, respectively (see the SI). Likewise, in the case of **P28H**, the direction of the induced ring current in the ACID map was also

reversed. From the calculated magnetic aromatic indices of hexaphyrins in the ground and triplet states, we can conceive that the aromaticity of hexaphyrins in the singlet excited state also becomes reversed with respect to that of the closed-shell singlet state.

Furthermore, to support the reversed aromaticity of **P26H** and **P28H** in the singlet excited state ( $Q_x$  state) relative to the closed-shell-singlet ground state, we estimated the HOMA values,<sup>3,4</sup> which can be a useful guide to the quantification of aromaticity in heteroatom-containing systems such as porphyrinoids, using the ground- and excited-state optimized structures calculated at the B3LYP/6-31G(d,p) level (see the SI). To analyze aromatic features according to the topological changes among the  $S_0$ ,  $T_1$ , and  $Q_x$  states in more detail, we computed the HOMA values for the main [26] and [28]  $\pi$ -conjugation pathways of **P26H** and **P28H** as illustrated in Chart 1, respectively (see the SI). Compared with the HOMA values for the ground states, those of the  $T_1$  state ( $0.80 \rightarrow 0.71$ ) and  $Q_x$  state ( $0.80 \rightarrow 0.78$ ) in **P26H** are reduced, while those of the  $T_1$  state ( $0.60 \rightarrow 0.79$ ) and  $Q_x$  state ( $0.60 \rightarrow 0.76$ ) in **P28H** are increased (see the SI). On the basis of the similar tendencies of the  $T_1$  and  $Q_x$  states and the instability of antiaromatic molecules that induces a change to nonaromatic ones via structural distortions, these results also support that the (anti)aromaticity of **P26H** and **P28H** is reversed in their singlet excited states. In addition, to clearly show the aromaticity reversal in the singlet excited states of **P26H** and **P28H** relative to their ground states, we evaluated the mean plane deviation, which represents the degree of structural distortion (Figure 3).<sup>34,35</sup> The mean plane deviation of **P26H**

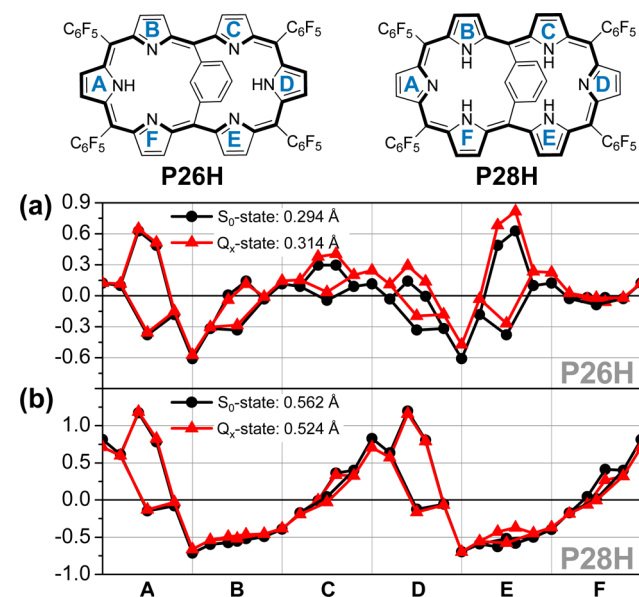


**Figure 3.** Mean plane deviation diagrams for (a) **P26H** and (b) **P28H** in the ground and singlet excited states based on their optimized structures.

in the ground state ( $0.294 \text{ \AA}$ ) is smaller than that in the  $Q_x$  state ( $0.314 \text{ \AA}$ ), which supports the aromaticity reversal of **P26H** in the  $Q_x$  state due to the structural distortion by antiaromaticity. In the case of **P28H**, on the other hand, the mean plane deviation is larger for the ground state ( $0.562 \text{ \AA}$ ) than for the  $Q_x$  state ( $0.524 \text{ \AA}$ ), which is well-matched with the above results as well. That is, these results also indicate that the



aromaticity and antiaromaticity of hexaphyrins in the  $S_0$  states are switched in their  $Q_x$  states. With these mean plane deviation values, the dihedral angles of bonds in the main  $\pi$ -conjugation pathways were investigated (see the SI). The mean values and standard deviations of the dihedral angles in the  $Q_x$  state of **P26H** ( $6.223^\circ$ ,  $7.403^\circ$ ) are larger than those in the ground state ( $6.170^\circ$ ,  $7.257^\circ$ ). In contrast to **P26H**, **P28H** shows decreased mean values and standard deviations of the dihedral angles in the  $Q_x$  state ( $7.623^\circ$ ,  $6.081^\circ$ ) relative to the ground state ( $7.968^\circ$ ,  $10.961^\circ$ ). In this regard, these aspects of the dihedral angle changes in the  $Q_x$  states were similarly observed in their  $T_1$  states. These results also imply that hexaphyrins show reversed aromatic features in the  $Q_x$  state relative to the  $S_0$  state, which is similar to their  $T_1$  state. Furthermore, these results are in good agreement with the previous theoretical works on simple annulenes such as benzene and cyclobutadiene in terms of the aromaticity reversal in the singlet excited states.<sup>26,27</sup>

In summary, the singlet-excited-state behaviors of Hückel aromatic and antiaromatic hexaphyrins observed from their TA spectra gave strong evidence of aromaticity reversal in their singlet excited states. These far-reaching results will provide us with useful information on the relationship between aromaticity and electronic structures and, as a consequence, on the chemical reactivity as well as the stability of porphyrinoids in their excited states.

## ■ ASSOCIATED CONTENT

### Supporting Information

The Supporting Information is available free of charge on the ACS Publications website at DOI: 10.1021/jacs.5b04047.

Experimental details, mathematical procedures, supporting tables and figures, and Cartesian coordinates (PDF)

## ■ AUTHOR INFORMATION

### Corresponding Authors

\*dongho@yonsei.ac.kr

\*osuka@kuchem.kyoto-u.ac.jp

### Notes

The authors declare no competing financial interest.

## ■ ACKNOWLEDGMENTS

The work at Yonsei University was supported by Samsung Science and Technology Foundation under Project SSTF-BA1402-10. The quantum calculations were performed using the supercomputing resources of the Korea Institute of Science and Technology Information (KISTI). The work at Kyoto University was financially supported by the Global Research Laboratory (GRL) Program (2013K1A1A2A0205183) funded by the Ministry of Education, Science and Technology (MEST) of Korea.

## ■ REFERENCES

- (1) Minkin, V. I.; Glukhovtsev, M. N.; Simkin, B. Y. *Aromaticity and Antiaromaticity: Electronic and Structural Aspects*; John Wiley & Sons: New York, 1994.
- (2) Cyrański, M. K. *Chem. Rev.* **2005**, *105*, 3773.
- (3) Krygowski, T. M.; Cyrański, M. K. *Chem. Rev.* **2001**, *101*, 1385.
- (4) Krygowski, T. M.; Cyrański, M. K. *Tetrahedron* **1999**, *55*, 11143.
- (5) Schleyer, P. v. R.; Maerker, C.; Dransfeld, A.; Jiao, H.; Hommes, N. J. R. v. E. *J. Am. Chem. Soc.* **1996**, *118*, 6317.
- (6) Buehl, M.; Thiel, W.; Jiao, H.; Schleyer, P. v. R.; Saunders, M.; Anet, F. A. L. *J. Am. Chem. Soc.* **1994**, *116*, 6005.

- (7) Cho, S.; Yoon, Z. S.; Kim, K. S.; Yoon, M.-C.; Cho, D.-G.; Sessler, J. L.; Kim, D. *J. Phys. Chem. Lett.* **2010**, *1*, 895.
- (8) Shin, J.-Y.; Kim, K. S.; Yoon, M.-C.; Lim, J. M.; Yoon, Z. S.; Osuka, A.; Kim, D. *Chem. Soc. Rev.* **2010**, *39*, 2751.
- (9) Rosenberg, M.; Dahlstrand, C.; Kilså, K.; Ottosson, H. *Chem. Rev.* **2014**, *114*, 5379.
- (10) Ottosson, H. *Nat. Chem.* **2012**, *4*, 969.
- (11) Baird, N. C. *J. Am. Chem. Soc.* **1972**, *94*, 4941.
- (12) Aihara, J. – i. *Bull. Chem. Soc. Jpn.* **1978**, *51*, 1788.
- (13) Gogonea, V.; Schleyer, P. v. R.; Schreiner, P. R. *Angew. Chem., Int. Ed.* **1998**, *37*, 1945.
- (14) Kataoka, M. *J. Chem. Res.* **2004**, *2004*, 573.
- (15) Feixas, F.; Vandenbussche, J.; Bultinck, P.; Matito, E.; Solà, M. *Phys. Chem. Chem. Phys.* **2011**, *13*, 20690.
- (16) An, K.; Zhu, J. *Eur. J. Org. Chem.* **2014**, 2764.
- (17) Wan, P.; Krogh, E. *J. Chem. Soc., Chem. Commun.* **1985**, 1207.
- (18) Wan, P.; Shukla, D. *Chem. Rev.* **1993**, *93*, 571.
- (19) Wörner, H. J.; Merkt, F. *Angew. Chem., Int. Ed.* **2006**, *45*, 293.
- (20) Möllerstedt, H.; Piqueras, M. C.; Crespo, R.; Ottosson, H. *J. Am. Chem. Soc.* **2004**, *126*, 13938.
- (21) Ottosson, H.; Kilså, K.; Chajara, K.; Piqueras, M. C.; Crespo, R.; Kato, H.; Muthas, D. *Chem. - Eur. J.* **2007**, *13*, 6998.
- (22) Rosenberg, M.; Ottosson, H.; Kilså, K. *Phys. Chem. Chem. Phys.* **2011**, *13*, 12912.
- (23) Jorner, K.; Emanuelsson, R.; Dahlstrand, C.; Tong, H.; Denisova, A. V.; Ottosson, H. *Chem. - Eur. J.* **2014**, *20*, 9295.
- (24) Sung, Y. M.; Yoon, M.-C.; Lim, J. M.; Rath, H.; Naoda, K.; Osuka, A.; Kim, D. *Nat. Chem.* **2015**, *7*, 418.
- (25) Ottosson, H.; Borbas, K. E. *Nat. Chem.* **2015**, *7*, 373.
- (26) Karadakov, P. B. *J. Phys. Chem. A* **2008**, *112*, 7303.
- (27) Karadakov, P. B. *J. Phys. Chem. A* **2008**, *112*, 12707.
- (28) Stepień, M.; Sprutta, N.; Latos-Grażyński, L. *Angew. Chem., Int. Ed.* **2011**, *50*, 4288.
- (29) Saito, S.; Osuka, A. *Angew. Chem., Int. Ed.* **2011**, *50*, 4342.
- (30) Sankar, J.; Mori, S.; Saito, S.; Rath, H.; Suzuki, M.; Inokuma, Y.; Shinokubo, H.; Kim, K. S.; Yoon, Z. S.; Shin, J.-Y.; Lim, J. M.; Matsuzaki, Y.; Matsushita, O.; Muranaka, A.; Kobayashi, N.; Kim, D.; Osuka, A. *J. Am. Chem. Soc.* **2008**, *130*, 13568.
- (31) Kim, K. S.; Yoon, Z. S.; Ricks, A. B.; Shin, J.-Y.; Mori, S.; Sankar, J.; Saito, S.; Jung, Y. M.; Wasielewski, M. R.; Osuka, A.; Kim, D. *J. Phys. Chem. A* **2009**, *113*, 4498.
- (32) Mori, H.; Lim, J. M.; Kim, D.; Osuka, A. *Angew. Chem., Int. Ed.* **2013**, *52*, 12997.
- (33) Geuenich, D.; Hess, K.; Köhler, F.; Herges, R. *Chem. Rev.* **2005**, *105*, 3758.
- (34) Suzuki, M.; Osuka, A. *Chem. Commun.* **2005**, 3685.
- (35) Cha, W.-Y.; Lim, J. M.; Yoon, M.-C.; Sung, Y. M.; Lee, B. S.; Katsumata, S.; Suzuki, M.; Mori, H.; Ikawa, Y.; Furuta, H.; Osuka, A.; Kim, D. *Chem. - Eur. J.* **2012**, *18*, 15838.